Surg Radiol Anat (1996) 18 : 89-96

Surgical and Radiologic Anatomy
Journal of Clinical Anatomy

Viscoelastic properties of human arteries Methodology and preliminary results

E Rosset[1], C Brunet[1], R Rieu[2], Ph Rolland[3], JF Pellissier[4], PE Magnan[5], P Foulon[6], A Drizenko[7], M Laude[6], A Branchereau[5] and A Friggi[3]

[1] Laboratoire d'Anatomie, Faculté de Médecine,[3] CJF 94-1 INSERM, Faculté de Pharmacie, 27, bd Jean Moulin, F-13005 Marseille, France
[2] Institut de Mécanique des Fluides, UM 34 - CNRS, Marseille, France
[4] Service d'Anatomo-Pathologie, Hôpital de la Timone, Marseille, France
[5] Service de Chirurgie Vasculaire, Hôpitaux Sud, F-13274 Marseille Cedex 9, France
[6] Laboratoire d'Anatomie d'Amiens, Faculté de Médecine, rue des Louvels, F-80036 Amiens Cedex, France
[7] Laboratoire d'Anatomie de Lille, Faculté de Médecine, 1, place de Verdun, F-59045 Lille Cedex, France

Abstract: In order to study the biomechanical properties of the arterial wall and to compare arteries with different histologic structures, we designed a device that allows testing of arterial segments under near-physiologic conditions. A hydrodynamic generator simulates systolo-diastolic pressures in an open loop. An intraarterial pressure sensor and a sonomicrometer connected to two piezoelectric crystals placed in diametric opposition on the arterial wall allow computer calculation of compliance, stiffness, midwall radial arterial stress, Young modulus, and incremental modulus for a given arterial segment at a given pressure setting. Seven healthy common carotid artery (CCA) segments and seven healthy (superficial) femoral artery (FA) segments were studied immediately after removal from brain-dead donors between the ages of 18 and 35 years. Histologic examination was performed to determine the density of elastic fibers in the arterial wall. Hysteresis was observed in all segments regardless of pressure settings. Compliance was greater and modulus values and stiffness were lower in CCA than in FA. No evidence of structural change was noted after testing in the circulation loop. These preliminary results open the way to a wide variety of applications for our hydrodynamic circulation loop. Experiments will be undertaken to compare the mechanical properties of arteries before and after cryopreservation.

Propriétés visco-élastiques des artères humaines. Méthodologie et résultats préliminaires

Résumé : Dans le but d'étudier les propriétés mécaniques de la paroi artérielle et de pouvoir établir des comparaisons entre des segments artériels de structure histologique différente, nous avons mis au point un banc d'essai hydrodynamique permettant de tester des segments artériels dans des conditions voisines de la réalité physiologique. Un générateur hydrodynamique permettait d'obtenir dans un circuit ouvert un régime de pressions de type systolo-diastolique. Un capteur de pression intra-artériel, ainsi qu'un sonomicromètre relié à des cristaux piézo-électriques placés de façon diamétralement opposée sur la paroi artérielle, permettaient de calculer, pour un régime de pressions donné et grâce à l'acquisition de données dans un système informatique, la compliance, la rigidité, la contrainte trans-pariétale, le module de Young, le module incrémentiel d'un segment artériel. Nous avons étudié sept artères carotides communes (CC), et sept artères fémorales (superficielles) (F) fraîchement prélevées chez des sujets sains âgés de 18 à 35 ans. Des corrélations avec la richesse en fibres élastiques de la paroi artérielle ont été établies. Nous avons mis en évidence un phénomène d'hystérésis pour chaque artère testée quel que soit le niveau de pression considéré. La compliance des artères CC a été plus importante, les modules et la rigidité ont été moins importants et ce de façon significative par rapport aux artères F. Aucune altération histologique n'a été mise en évidence après passage des segments artériels au banc d'essai. Ces résultas préliminaires nous permettent d'envisager de nombreuses applications à ce travail dont l'une d'entre elles sera la mesure comparative des propriétés mécaniques des artères avant et après cryopréservation.

Key words: Arteries — Man — Biomechanics

Correspondence to : E Rosset

Arterial walls display specific mechanical properties that enable them to fulfil their crucial role in the circulatory system, i.e. providing continuous flow of blood to tissues. These properties are due mainly to viscoelastic mechanisms that allow arteries to maintain perfusion pressure by adjusting their diameter. Since these mechanisms depend on the structure of the artery, changes in the arterial wall can adversely affect blood supply to downstream tissues [21]. Arterial wall structure varies according to anatomic location. Traditionally arteries have been divided into two categories: elastic arteries such as the common carotid artery (CCA) and muscular arteries such as the (superficial) femoral artery (FA) [13]. This structural heterogeneity together with the strict dependence of commonly measured mechanical parameters on physiologic factors such as heart rate, intraarterial pressure, and smooth muscle cell activation hinders in vivo assessment of the mechanical properties of human arteries [21]. A number of in vitro studies have been conducted but the most interesting results concern animal arteries.

The purpose of this study was to test a new mock circulation loop designed to allow reproducible measurement of the mechanical properties of arterial substitutes under near-physiologic conditions without altering the structure of the test segment.

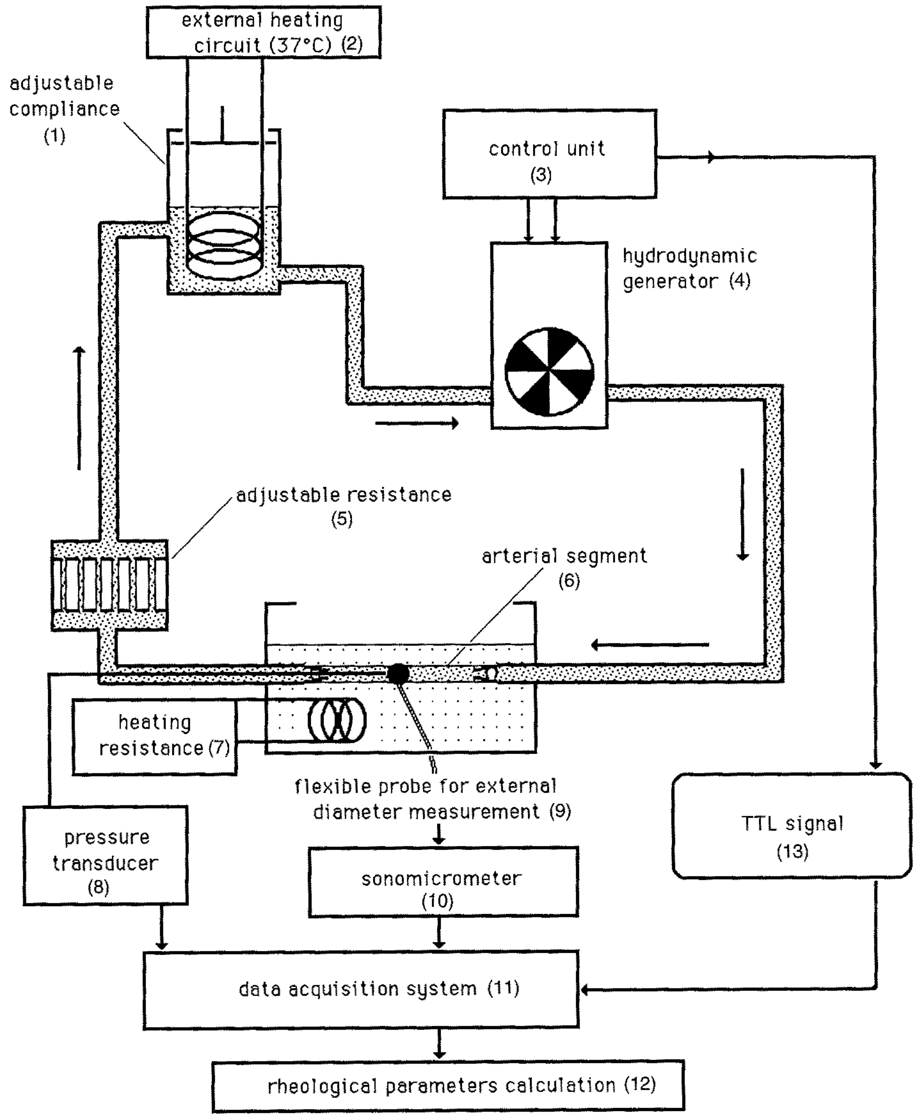

Fig. 1
Drawing showing the mock circulation loop used to test arterial segments in this study. *1,* adjustable compliance ; *2,* external heating circuit (37°C) ; *3,* control unit ; *4,* hydrodynamic generator ; *5,* adjustable resistance ; *6,* arterial segment ; *7,* heating resistance 37°C ; *8,* pressure transducer ; *9,* flexible probe for external diameter measurement (SEDUC) ; *10,* sonomicrometer ; *11,* data acquisition system ; *12,* rheological parameters calculation ; *13,* TTL signal

Schéma général du banc de simulation d'écoulement physiologique sur lequel ont été testés les segments artériels. *1,* compliance ajustable ; *2,* circuit externe de réchauffament (37°C) ; *3,* asservissement ; *4,* pompe ; *5,* resistance ajustable ; *6,* segment d'artère ; *7,* circuit thermostaté à 37°C ; *8,* transducteur de pression ; *9,* sonde souple (SEDUC) ; *10,* sonomicromètre ; *11,* chaine d'acquisition des données ; *12,* calcul des paramètres rhéologiques artériels ; *13,* signal de synchronisation de la pompe pour le déclenchement de l'acquisition

Material and methods

Test segments

Arterial segments were removed during multiple organ harvesting in patients declared brain-dead in accordance with then prevailing laws. Seven FA and seven CCA were taken from five different donors including three men and two women, with a mean age of 24.2 years. To allow mounting in the mock circulation loop at the same length as *in situ*, segments were measured before division using a flexible tape measure. Thin suture (monofilament 6/0) or clips were used to mark the end-points. Immediately after removal, the arteries were placed in a cell culture medium (RPMI 1640) with antibiotics. The composition of the solution was identical to that of clinically used solutions [10]. The bottle was placed in a container with crushed ice and immediately taken to the laboratory. All tests were performed within 24 hours after removal. Before mounting in the mock circulation loop, the segments were prepared as follows. The diameter of the lumen was measured. The arterial wall was inspected to ensure the absence of lesions, tears, or leaks. Collaterals were ligated using clips or 6/0 monofilament suture. The chosen segments were as straight as possible and the diameter of the lumen as regular as possible. The *in situ* length of the segments ranged from 4 to 12 cm (mean: 8.7 cm).

Mock circulation loop

Our test system was composed of an open hydraulic loop with a hydrodynamic generator that simulated physiologic systolo-diastolic pressures. The generator comprised a triphase electric motor driving a volumetric gear pump via two counter-rotative clutches. The main components of the electronic assembly were the control signal generator, the entry signal amplifier, a comparer, and two current amplifiers set in opposite phase supplying the clutches. A tachymetric dynamo on the pump axis was used to monitor the pumping cycle [9, 16, 18]. The hydraulic circuit is depicted in Fig. 1. Ringer lactate was used to fill the circuit because it is an isotonic solution with optimal ionic composition and pH for preservation of cell membranes. Temperature was maintained at 37°C using an external warming circuit. The arterial segments were mounted in the mock circulation loop using two sliding connectors with cone shaped tips for arteries of different diameter. After attachment using a braided suture, the segment was adjusted to the in situ length and the tub was filled with Ringer lactate. When full, the external peri-arterial pressure was similar to that provided by interstitial tissue (less than 5 cm H_20).

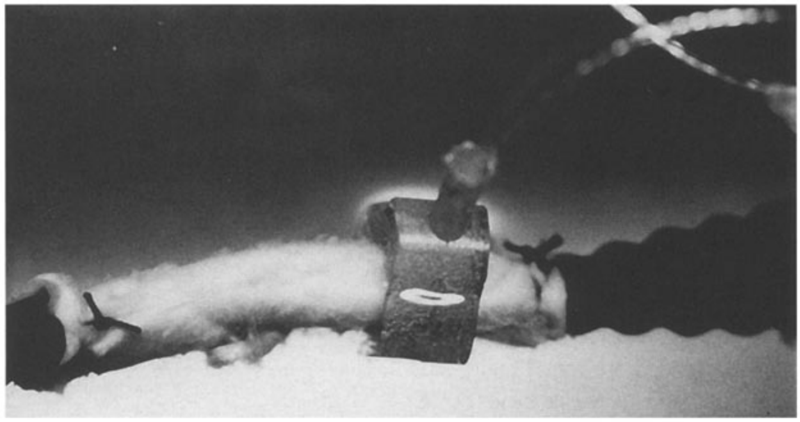

Fig. 2
(Superficial) femoral a. mounted in the mock circulation loop. One collateral has been closed using a clip. The SEDUC catheter is in place and connected to the sonomicrometer
Artère fémorale montée sur le banc d'essai. Une branche collatérale a été aveuglée par un clip. La sonde SEDUC reliée à un sonomicromètre est en place

Measurements

Intraarterial pressure and external diameter were measured simultaneously. These measurements were made as close to the middle of the artery as possible, depending mainly on the presence of ligated collaterals. Real-time and mean arterial pressures were measured using a 5F "Millar" MPC-500 pressure microcatheter introduced through one of the connectors using a "T" adaptor. The hydrodynamic generator simulated systolo-diastolic pressures with a pulse rate of 60 beats per minute. To allow comparison of results, the same systolo-diastolic pressure differential (60 mmHg) and incremental pressure (30 mmHg) were used in all experiments. In this study the following four pressure settings were used: 50-110 mmHg, 80-140 mm Hg, 110-170 mmHg, and 140-200 mmHg.

Variations in the external diameter of the artery during pulsations were measured using an ultrasound technique. Diameter was calculated in function of the time necessary for ultrasound signals (5 MHz) to pass between two piezoelectric crystals (emitter and receiver) located in diametric opposition in a flexible silastene catheter ("SEDUC" : Dimensional Assessment Catheter for Clinical Use made by CJF-INSERM 94-1). The catheter is available in a number of sizes so that it can be fitted to the artery without altering hindering or impeding the wall (Fig. 2).

A synchronisation signal (TTL) from the generator controlling the pump was used to trigger data acquisition by the computer. After amplification and filtration, signal data were recorded on audiotape using a Bio-Logic DTR 1800® multitrack analog recorder. Analysis of data was performed after analog-digital conversion on a Hewlett-Packard Vectra® computer. The software used to process physiologic signals can calculate means with data from 20 cycles (i.e. every 20 s). Recordings were performed at least five minutes after starting the circulation device. After testing, the artery was removed from the loop and a 2 cm segment (*in situ* length) was cut off, weighed (Mettler® scale, sensitive to the mg), and used to allow calculation of the internal radius and thickness [15].

Measurements and calculated parameters

The following direct measurements were made:

- intraarterial systolic pressure (Psyst);
- intraarterial diastolic pressure (Pdiast);
- mean pressure (Pm);
- external systolic diameter (Ds);
- external diastolic diameter (Dd);
- mean diameter (Dm).

The measured data were used to calculate the following parameters:

- arterial pulsatility (ΔD) and relative pulsatility ($\Delta D/Dm$)
- compliance (Co) according to the formula:

$$Co = \Delta V/\Delta P)$$

where ΔV is the variation of the internal diameter of the artery and ΔP is the pressure differential. Compliance is a measure of wall elasticity, ie the ability of the wall to expand in terms of a given volume of blood depending on the pressure. Compliance is expressed in $ml.mmHg^{-1}.10^{-3}$.

- stiffness (AoS) according to the formula:

$$AoS = \Delta P/\Delta D$$

Stiffness is a measure of the variation of external diameter in terms of the pressure change. Stiffness can be considered as the opposite of compliance and is expressed in mm $Hg.cm^{-1}$ [19].

midwall radial arterial stress (σ) according to the formula:

$\sigma = 2.P$ (diast or syst)$.(ab/R)^2/(b^2-a^2)$

where a is the internal diameter of the artery, b is the external radius, R is the mean radius, ie (a + b)/2, and P is arterial pressure. As indicated, this formula allows calculation of both systolic (σ syst) and diastolic (σ diast) midwall radial arterial stress. Mean midwall radial stress calculated from σ syst and σ diast is a measure of the internal and external stress applied to the arterial wall. Mean midwall radial stress is expressed in $KN.m^{-2}$ [15].

- Young's modulus (Ep) according to the formula

$$Ep = \Delta P/\Delta D).(D/h)$$

where ΔP is the pressure variation, ΔD is the diameter variation, Dm is mean diameter, and h is mean wall thickness. Young's modulus is a measure of the ratio between stress and resulting deformation and is expressed in mmHg cm^{-1} [14].

- incremental modulus (Einc) calculated according to the formula

$$Einc = 0.75\ R\ (\Delta\sigma/DR)$$

where $\Delta\sigma$ is the difference between σ syst and σ diast. Incremental modulus is a measure of the elasticity of the wall and represents a linear function of stress. Incremental modulus is expressed in $kN.m^{-2}$ [7, 15].

Histology

After harvesting and weighing, a short piece of the arterial segment was placed in Bouin's fluid pending histologic study. Several staining methods were used: HPS (hematoxylin, phloxin, safran) or HES (hematoxylin, eosin, safran) for routine examination of arterial walls, Masson Trichrome green for study of collagen fibers and cell nuclei, and orcein for determination of elastic fiber density. Particular attention was paid to detect any alteration in the structure of the arterial wall.

Results

Pressure/diameter curves were plotted for each artery. Hysteresis was observed in all tests, proving that the viscoe-

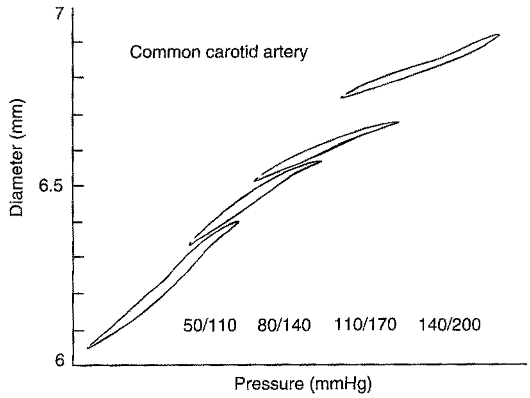

Fig. 3
Pressure-diameter curve for a common carotid a. at four pressure settings. The amplitude of hysteresis and the slope of the curve are consistent with the high compliance expected in elastic arteries

Courbe pression-diamètre d'une artère carotide commune aux quatre niveaux de pression testés. Noter l'amplitude du phénomène d'hystérésis et la pente de la courbe traduisant la compliance élevée des artères de type élastique

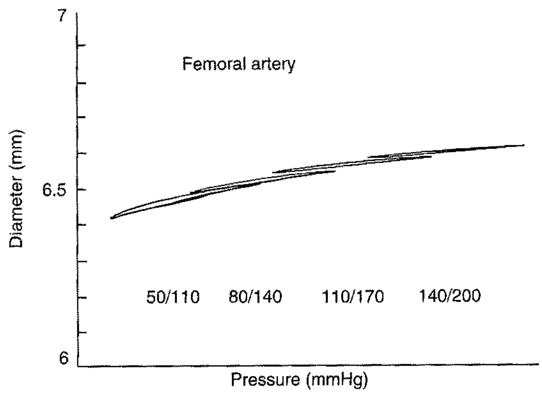

Fig. 4
Pressure-diameter curve for a (superficial) femoral a. at four pressure settings. The lower amplitude of hysteresis and lesser slope of the curve are consistent with the lesser compliance expected in muscular aa. as compared to elastic arteries

Courbe pression-diamètre d'une artère fémorale aux quatre niveaux de pression testés. L'hystérésis est ici moins important de même que la pente de la courbe traduisant la rigidité plus importante des artères de type musculaire

Table 1. Main rheologic parameters measured in common carotid arteries (n = 7) at 4 pressure settings
Principaux paramètres rhéologiques de l'a. carotide commune (n = 7) dans les 4 gammes de pression

Parameter	50 - 11 mmHg	80 - 140 mmHg	110 - 170 mmHg	140 - 200 mmHg
ΔD (mm x 10^{-3})	592 ± 49	451 ± 50*	272 ± 37*	184 ± 33*
$\Delta D/Dm$ (%)	8.56 ± 0.67	6.05 ± 0.63*	3.50 ± 0.42*	2.48 ± 0.40*
Co (ml $mmHg^{-1}$ x 10^{-3})	1169 ± 111	944 ± 119*	598 ± 89*	423 ± 85*
σ (KN m^{-2})	42.4 ± 3.4	70.0 ± 6.4*	97.7 ± 8.7*	127.5 ± 11.2*
Ep ($mmHgcm^{-1}$)	96 ± 12	146 ± 30*	268 ± 36*	435 ± 67*
Einc (kN m^{-2})	302 ± 38	491 ± 103*	917 ± 117*	1349 ± 233*
AoS ($mmHgcm^{-1}$)	994 ± 81	1338 ± 162*	2290 ± 289*	3505 ± 477*

ΔD: arterial pulsatility; *ΔD/Dm*: arterial pulsatility vs mean diameter; *Co*: compliance; *σ*, midwall radial arterial stress; *Ep*: Young modulus; *Einc*: incremental modulus; *AoS*: stiffness. Values are means ± SEM.
* Measured or calculated values significantly different ($p<0.05$) from corresponding values measured or calculated at lower pressure setting

ΔD, pulsatilité artérielle ; *ΔD/Dm*, pulsatilité artérielle vs diamètre moyen ; *ho/R*, épaisseur moyenne de l'artère vs le rayon moyen ; *Co*, compliance aortique ; *σ*, contrainte radiale transpariétale ; *Ep*, module élastique de Young ; *Einc*, module d'élasticité incrémentiel ; *AoS*, rigidité aortique. Les valeurs indiquées sont les moyennes ± SEM. *valeurs mesurées ou calculées significativement différentes ($p<0.05$) des mêmes valeurs mesurées ou calculées dans les gammes de pression inférieures

Table 2. Main rheologic parameters measured in superficial femoral arteries (n = 7) at 4 pressure settings
Principaux paramètres rhéologiques de l'a. fémorale (superficielle) (n = 7) dans les 4 gammes de pression

Parameter	50 - 11 mmHg	80 - 140 mmHg	110 - 170 mmHg	140 - 200 mmHg
ΔD (mm x 10^{-3})	243 ± 35	139 ± 19*	99 ± 13*	78 ± 11*
ΔD/Dm (%)	4.14 ± 0.56	2.29 ± 0.30*	1.61 ± 0.21*	1.24 ± 0.19*
Co (ml $mmHg^{-1}$ x 10^{-3})	449 ± 68	263 ± 36*	193 ± 25*	156 ± 22*
σ (KN m^{-2})	46.2 ± 6.0	68.4 ± 8.1*	91.4 ± 9.8*	116 ± 13.0*
Ep ($mmHgcm^{-1}$)	266 ± 53	479 ± 83*	697 ± 131*	939 ± 188*
Einc (kN m^{-2})	698 ± 158	1127 ± 237*	1910 ± 400*	2636 ± 581*
AoS ($mmHgcm^{-1}$)	2610 ± 385	4451 ± 581*	6171 ± 854*	7940 ± 1175*

ΔD: arterial pulsatility; *ΔD/Dm*: arterial pulsatility vs mean diameter; *Co*: compliance; *σ*, midwall radial arterial stress; *Ep*: Young modulus; *Einc*: incremental modulus; *AoS*: stiffness. Values are means ± SEM. * Measured or calculated values significantly different ($p<0.05$) from corresponding values measured or calculated at lower pressure setting

ΔD, pulsatilité artérielle ; *ΔD/Dm*, pulsatilité artérielle vs diamètre moyen ; *ho/R*, épaisseur moyenne de l'artère vs le rayon moyen ; *Co*, compliance aortique ; *σ*, contrainte radiale transpariétale ; *Ep*, module élastique de Young ; *Einc*, module d'élasticité incrémentiel ; *AoS*, rigidité aortique. Les valeurs indiquées sont les moyennes ± SEM. *valeurs mesurées ou calculées significativement différentes ($p<0.05$) des mêmes valeurs mesurées ou calculées dans les gammes de pression inférieures

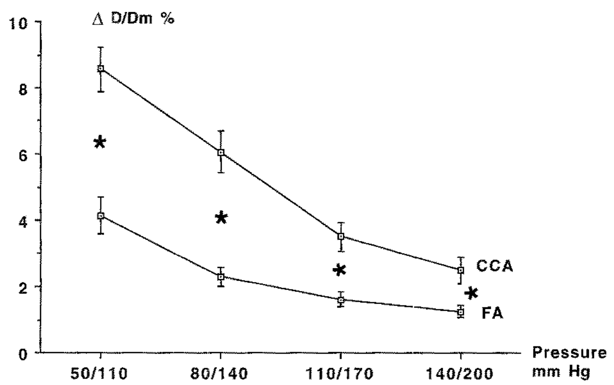

Fig. 5
Comparison of arterial pulsatility (*ΔD/Dm*) in common carotid aa. (*CCA*) and (superficial) femoral aa. (*FA*). Stars indicate statistically significant differences (Student test; $p < 0.05$)

Valeurs de la pulsatilité artérielle (*ΔD/Dm*) pour les aa. carotides communes (*CC*) et les aa. fémorales (*F*). Les étoiles indiquent les différences significatives sur le plan statistique (test de Student, p<0,05)

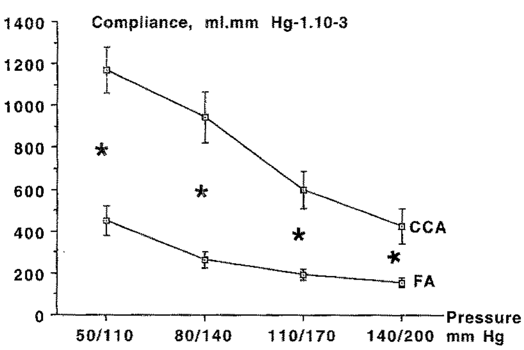

Fig. 6
Comparison of arterial compliance (*Co*) in common carotid aa. (*CCA*) and (superficial) femoral aa. (*FA*). Stars indicate statistically significant differences (Student test; $p < 0.05$)

Valeurs de la compliance artérielle (*Co*) pour les aa. carotides communes (*CC*) et les aa. fémorales (*F*). Les étoiles indiquent les différences significatives sur le plan statistique (test de Student, p<0,05)

lastic properties of the arterial wall were preserved at all four pressure settings (Fig. 3 and 4). The amplitude of hysteresis was much greater for elastic arteries (CCA) than for muscular arteries (FA). Rheologic parameters calculated for CCA and FA at the four pressure settings are summarised in Tables 1 and 2 respectively. Significant differences in pulsatility, compliance, stiffness, midwall radial arterial stress, Young's modulus, and incremental modulus were observed in arteries of the same type (CCA or FA) from one pressure setting to another. The curves in Figures 5 to 10 compare pulsatility, compliance, stiffness, Young's modulus, incremental modulus, and midwall radial arterial stress in the two types of arteries at each pressure setting. Significant differences in pulsatility, compliance, stiffness, Young's modulus, and incremental modulus were observed between the two types of arteries (CCA and FA) at each pressure setting. There was no significant difference between CCA and FA with regard to midwall radial arterial stress.

Histologic examination showed no sign of any alteration in arterial wall structure after testing. The different layers of the artery were intact. Orcein staining allowed determination of the elastic fiber density. The CCAs always displayed more elastic fibers than the FAs (Figs. 11 and 12). Scanning electron microscopy showed that testing in the mock circulation loop did not damage the arterial endothelium (Fig. 13).

Discussion

Test device

The mock circulation device that we designed provided near-physiologic pressure levels, pressure differential, pulse rate and temperature. It also allowed arteries to be tested at their in situ length, thus taking into account the anatomic changes described by Learoyd and Taylor [12] who reported that arteries tend to retract less with age and that the extent of retraction was inversely related to the distance of the artery from the heart. In their study, these authors estimated arterial retraction in young subjects (under 35 years) to be between 25 and 40%, a range comparable with the one observed in this study. Variation in rheologic parameters with age has been documented by a number of other authors [12, 15, 20]. To avoid ageing as a possible bias in this study, we included only young subjects according to the definition of Learoyd and Taylor [12], i.e. under 35 years. Our results were homogeneous.

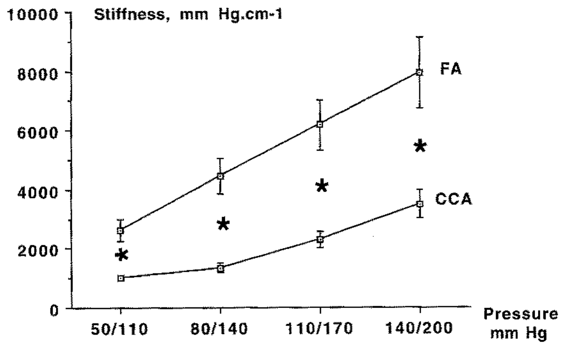

Fig. 7
Comparison of stiffness (*Aos*) in common carotid aa. (*CCA*) and (superficial) femoral aa. (*FA*). Stars indicate statistically significant differences (Student test; $p < 0.05$)

Valeurs de la rigidité artérielle (*Aos*) pour les aa. carotides communes (*CC*) et les aa. fémorales (*F*). Les étoiles indiquent les différences significatives sur le plan statistique (test de Student, p<0,05)

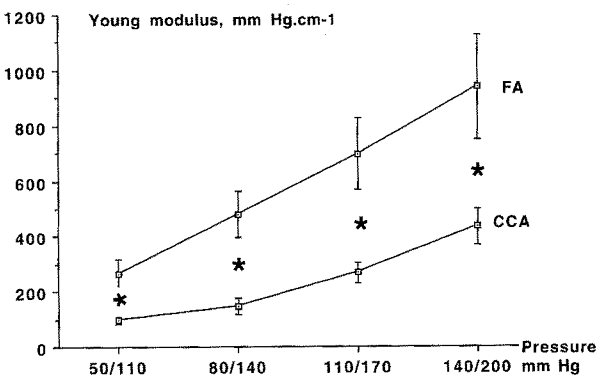

Fig. 8
Comparison of Young's modulus (*Ep*) in common carotid aa. (*CCA*) and (superficial) femoral aa. (*FA*). Stars indicate statistically significant differences (Student test; $p < 0.05$)

Valeurs du module de Young (*Ep*) pour les aa. carotides communes (*CC*) et les aa. fémorales (*F*). Les étoiles indiquent les différences significatives sur le plan statistique (test de Student, p<0,05)

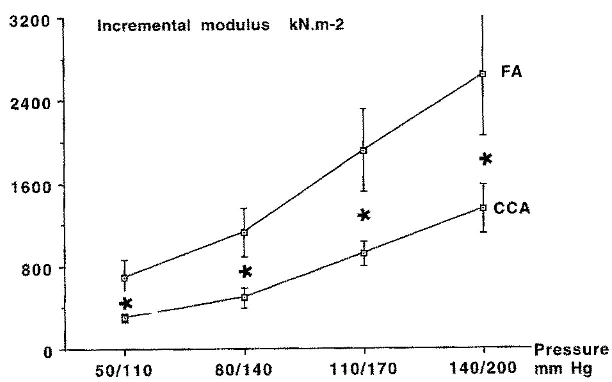

Fig. 9. Comparison of incremental modulus (*Einc*) in common carotid aa. (*CCA*) and (superficial) femoral aa. (*FA*). Stars indicate statistically significant differences (Student test; $p < 0.05$)

Valeurs du module incrémentiel (*Einc*) pour les aa. carotides communes (*CC*) et les aa. fémorales (*F*). Les étoiles indiquent les différences significatives sur le plan statistique (test de Student, p<0,05)

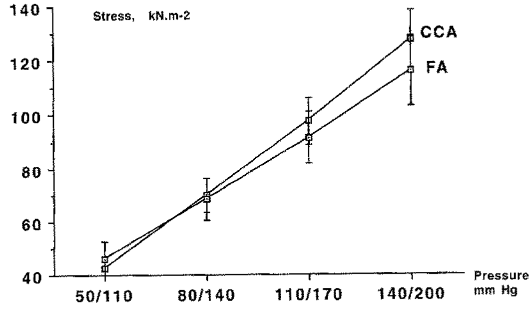

Fig. 10. Comparison of midwall radial arterial stress (σ) in common carotid aa. (*CCA*) and (superficial) femoral aa. (*FA*). Stars indicate statistically significant differences (Student test; $p<0.05$)

Valeurs de la contrainte trans-pariétale (σ) pour les aa. carotides communes (*CC*) et les aa. fémorales (*F*). Nous n'avons pas observé de différence significative entre les CC et les F, la contrainte étant surtout dépendante de la pression intra-artérielle

Experimental handling was done under sterile conditions up to testing in the mock circulation loop. Harvesting, transport, and preparation of the artery were performed under standard operating-room aseptic conditions, thus minimising the risk of bacterial contamination of the arterial wall. Aseptic conditions could not be maintained in the mock circulation loop because it is not easy to disinfect the whole test device. However it seems unlikely that contamination during the 30 to 45 min necessary to mount the artery in the test device and record experimental data was sufficient to alter the mechanical properties of the arteries. The duration of storage at 4° C prior to testing was kept as short as possible to avoid structural changes. In this regard, Abebe et al [1] observed extensive edema and damage to intracellular organelles after 24 h at +4° C. However, it should be emphasized that these authors used Eurocollins as the preservative medium whereas we preferred RPMI 1640. RPMI 1640 is a culture medium that allows prolonged preservation (1 to 21 days) of human arteries [10]. Kirklin et al [11] emphasized the possible toxicity of prolonged soaking in solution containing high concentrations of antibodies. To protect our segments from this type of damage, we minimized the duration of soaking in antibiotic solution.

Since the SEDUC® catheter used to measure variations in arterial diameter is flexible and light, it does not hinder or impede the arterial wall in any way. The variation in relative pulsatility ($\Delta D/Dm$) was between 4% for FA to 10% for CC. These variations are comparable to those observed when measurements were made with optical techniques [5]. Another advantage of the SEDUC® catheter is that it can be used to hold the piezoelectric sensors against the external surface of the artery in diametric opposition. Sensors were placed at different diameters (mm by mm) so that the catheter could be replaced if the diameter of the artery changed greatly as the pressure setting was increased. Measurements obtained using the catheter to hold the sensors were similar to those obtained when the sensors were attached to the arterial wall using fibrin

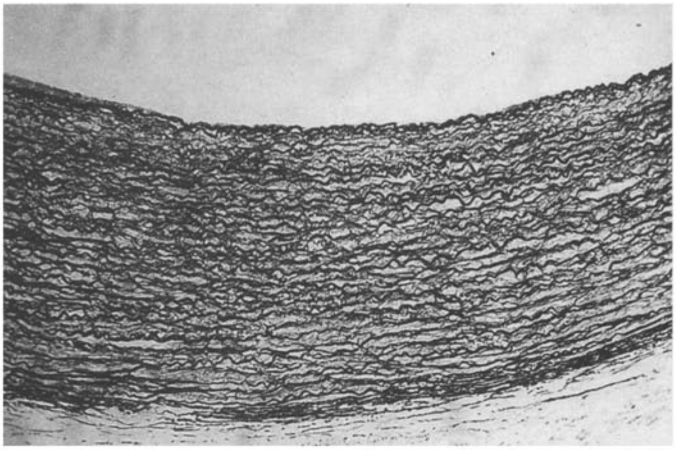

Fig. 11. microscopic view of a common carotid a. after orcein staining (x100). Note the intact structure of the arterial wall and the high density of elastic fibers

A. carotide commune, microscopie optique x 100, coloration par l'orcéïne. Noter l'intégrité architecturale de la paroi artérielle et la haute densité en fibres élastiques

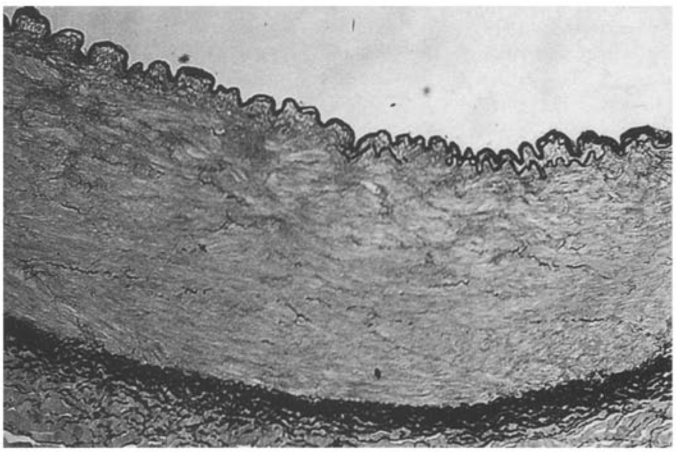

Fig. 12. Microscopic view of (superficial) femoral a. after orceine staining (x100). Note the intact structure of the arterial wall and the low density of elastic fibers

A. fémorale, microscopie optique x 100, coloration par l'orcéïne. Noter ici aussi l'intégrité architecturale de la paroi artérielle et la rareté des fibres élastiques

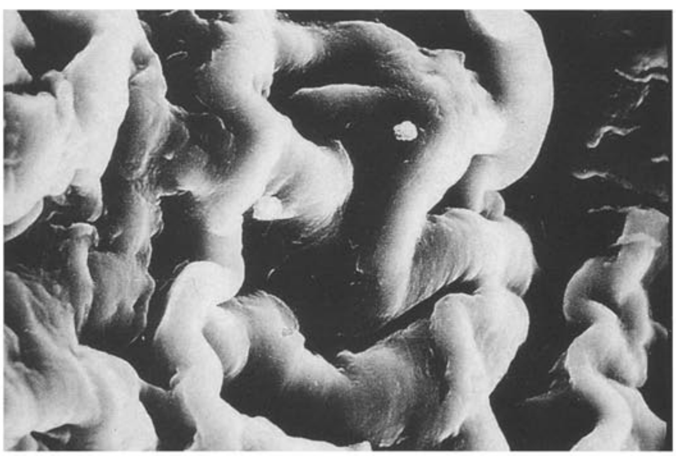

Fig. 13. Scanning electron microscopic view of (superficial) femoral a. (x1000). Note that the vascular endothelium was not damaged by testing in our mock circulation loop

A. fémorale, microscopie à balayage x 1000. Noter l'intégrité de l'endothélium vasculaire après passage du segment artériel dans le banc de simulation

glue [3]. Positioning the sensors with the catheter rules out the possibility of the sensor becoming detached during the test or the problems associated with having to glue or sew on two captors in diametric opposition.

Our test device does not damage the structure of the arteries. Histologic study of tested arteries revealed no zone of necrosis or structural change able to jeopardise mechanical properties. The results demonstrated a strong correlation between histologic structure and mechanical performance, with arteries having the highest density of elastic fibers such as the CCA having significantly better compliance than muscular arteries such as the FA.

Rheologic properties of arteries

Hysteresis was observed in all arteries tested, regardless of the pressure setting. Previous reports indicated that hysteresis was greater at the beginning of the test [2, 5]. This enhancement is related to the extensible nature of the arterial wall as documented by Remington [17], who reported that the width of the hysteresis loop was dependent on how much the artery is stretched. To avoid bias due to this phenomenon, we waited for the pressure/diameter response to stabilise before recording data. Figures 3 and 4 show that the hysteresis also depends on the density of elastic fibers in the arterial wall with the amplitude of the loop being much greater for CCA than for FA. The steeper slope of the loop at low pressure settings was probably due to incomplete recruitment of elastic fibers. The lessening of the slope at high pressure settings may have been due to recruitment of collagen fibers [6]. Obviously harvesting of arteries leads to complete denervation and as a result the tested artery is an inert conduit. This eliminates any bias due to neurogenic stimuli that might occur during in vivo tests. The possibility of contraction of smooth muscle cells due to an extracellular and intracellular electrolyte imbalance was ruled out by the fact that injection of papaverine into the loop and arterial wall did not cause any change in the diameter of the artery.

Conclusion

Our mock circulation loop allows reliable assessment of the rheologic characteristics of arteries without wall damage. In the present study we were able to measure the main parameters of arterial segments with different histologic structure. Our goal is to study arteries from all over the body in order to draw a rheologic map of the circulatory network. The test device has many other applications, eg evaluating the mechanical properties of cryopreserved arteries or other arterial substitutes used for surgical bypass (saphenous veins, prostheses, and bioprostheses).

References

1. Abebe W, Cavallari N, Agrawal DK, Rowley J, Thorpe PE, Hunter WJ, Edwards JD (1993) Functional and morphological assessment of rat aorta stored in University of Wisconsin and Eurocollins solutions. Transplantation 56 : 808-816
2. Bergel DH (1961) The static elastic properties of the arterial wall. J Physiol 156 : 445-457
3. Charpiot P, Rolland PH, Friggi A, Piquet P, Scalbert E, Bodard H, Barlatier A, Latrille V, Tranier P, Mercier C, Luccioni R, Calaf R, Garçon D (1993) Angiotensin converting enzyme inhibition with periindopril and atherogenesis induced structural and functional changes in mini-pig arteries. Arterioscler Thromb 13 : 1125-1138
4. Cox RH (1975) Anisotropic properties of canine carotid artery in vitro. J Biomechanics 8 : 293-300
5. Dobrin PB (1978) Mechanical Properties of Arteries. Physiol Rev 58 : 397-460
6. Dobrin PB (1990) Physiopathologie et pathogénie des anévrysmes de l'aorte abdominale. In : Kieffer E (ed) Les anévrysmes de l'aorte abdominale sous-rénale. AERCV, Paris, pp 9-21
7. Friggi A, Bodard H, Berenger FP, Esclapez F, Rolland PH (1989) Effects of sin-1 on peripheral hemodynamics and viscoelastic properties of aorta in anesthetized rabbits. Cardiovasc Drugs Ther 3 : 445-458
8. Gow BS (1970) Viscoelastic properties of conduit arteries. Circ Res 26 [Suppl II] : 113-122
9. Issartier P, Siouffi M, Pelissier R (1978) Simulation of blood flow by a hydrodynamic generator. Med Prog Technol 6 : 39-40
10. Kieffer E., Bahnini A, Koskas F, Ruotolo C, Le Blevec D, Plissonnier D (1993). In situ allograft replacement of infected infrarenal aortic prosthetic grafts: results in forty-three patients. J Vasc Surg 17 : 349-356
11. Kirklin JK, Smith D, Novick W, Naftel DC, Kirlin JW, Pacifico AD, Nanda NC, Helmcke FR, Bourge RC (1993) Long-term function of cryopreseved aortic homografts. J Thorac Cardiovasc Surg 106 : 154-166
12. Learoyd BM, Taylor MG (1965) Alterations with age in the viscoelastic properties of human arterial walls. Circ Res 16 : 278-292
13. Maillet M (1989) Histologie des artères de moyen et grand calibre. In : Rouffy J, Natali J (eds) Artériopathies périphériques non athéromateuses. Masson, Paris, pp 36-55
14. Nichols WW, O'Rourke MF (1990) Properties of the arterial wall. In: Mc Donald's (ed) Blood flow in arteries. Arnold, London, pp 77-124
15. Pagani M, Mirsky I, Baig H, Manders WT, Kerkhof P, Vatner SF (1979) Effects of age on aortic pressure. Diameter and elastic stiffness. Stress relationships in unanesthetized sheep. Circ Res 44 : 420-429
16. Pelissier R, Cassot F, Farahifar D, Bialonski W, Issartier P, Bodard H, Friggi A (1983) Simulateur cardiovasculaire. ITBM 4 : 33-45
17. Remington JW (1955) Hysteresis loop behavior of the aorta and other extensible tissues. Am J Physiol 180 : 83-95
18. Rieu R, Friggi A, Farahifar D, Cassot F (1987) Determination in vitro de la relation pression-diamètre et des profils de vitesse par des techniques ultrasonores. Application in vivo. J Physiol (Paris) 82 : 175-182
19. Sauer G, Tebbe U, Krause H (1981) Die Wirkung von Molsidomin auf den arteriellen "Windkessel». Z Kardiol 70 : 713-718
20. Sonesson B, Hansen F, Stale H, Lanne T (1993) Compliance and Diameter in the human abdominal aorta. The influence of age and sex. Eur J Vasc Surg 7 : 690-697
21. Tedgui A, Lévy B (1994) Biologie de la paroi artérielle. Masson, Paris

Received September 4, 1995 / Accepted in final form February 15, 1996